NUMERICAL SIMULATION OF THERMOPHORETIC PARTICLE DECONTAMINATION IN CLEAN ROOMS

Jong Ho Lee, Won Seok Moon and Seung Bin Park[†]

Dept. of Chemical Engineering, KAIST, 373-1 Kusong-dong, Yusong-gu, Taejon 305-701, Korea

Abstract—In order to develop strategies for minimizing deposition of contaminant particles of diameters ranging from 0.1 to 1.0 µm on a wafer, the effect of thermophoresis on a particle deposition velocity was numerically studied. The angle between wafer surface and direction of free-stream flow was introduced as a system parameter. Convection, diffusion, sedimentation, and thermophoresis were included as particle transport mechanisms. Similarity transform was applied to the model equations and obtained equations with dimensions reduced by one. The results suggest that it is possible to enhance the removal of particles of diameter ranging from 0.1 to 1.0 µm by heating with a temperature difference of 10-30℃ between wafer surface and the air stream. If the filter of a clean room removes well around 0.1 µm sized particles, the free-stream velocity or flow angle should be increased for the effective removal of particle by thermophoresis, but, if the filter is efficient in removing particles around 1 µm, the free-stream velocity or flow angle should be decreased.

Key words: Thermophoresis, Clean Room, Particle Deposition, Particle Decontamination, Wafer Surface

INTRODUCTION

Contamination by particle deposition onto wafer surface during manufacturing steps is a major cause of yield loss of semiconductor product in the micro-electronics industry [Harrigan and Stoller, 1991], and it becomes more serious as the feature size of the product becomes smaller. It is known that over 75% of yield loss results from the contamination by the particle in case feature size of the micro-circuit is below 1 µm [Davis et al., 1993]. The contamination by the particle deposition is also a problem in the production of optical fiber or pharmaceuticals as well as semiconductor devices.

There are two main sources of contaminant particles. One source is rather external one, i.e., the clean room air, process gas, people in the clean room, and the other one is the particle which is generated inside the CVD reactor by physical and chemical processes [Davis et al., 1993]. Practically, the particles of diameter ranging from 0.1 to 1.0 µm are considered as the most critical [Bae et al., 1994].

The removal of the contaminant by filtering is relatively efficient in the particles larger than 1 µm and smaller than 0.1 µm. This is because the sedimentation or inertia force is dominant in the system of particles larger than 1 µm, and diffusional transport is very efficient in the system of particles smaller than 0.1 µm. On the other hand, particles of intermediate size of which diameter ranging from 0.1 to 1.0 µm are most difficult to remove because diffusion and sedimentation or inertia force do not work significantly on the these particles. However, experimental data for deposition velocity of these particles are very rare and existing data are not reliable due to the lack of reproducibility. The dominant transport mechanisms of these particles include thermophoresis as well as sedimentation and diffusion. Thermophoresis is a phenomenon by which suspended particles migrate from hot

region to cold region when the temperature gradient exists in suspension medium [Reist, 1993].

Flow field around the wafer should be characterized and particle transport mechanisms should be considered to make up strategies for minimizing particle deposition. Then particle deposition flux onto wafer surface can be calculated with these informations and it can be minimized by controlling appropriate parameters. For this reason, various studies dealing with particle dynamics and deposition have been performed over the dynamics of particles of diameter ranging from 0.01 to oder of 10 µm.

Stratmann et al. [1987] considered only thermophoresis as the particle transport mechanism under the condition of stagnation flow on a infinite plane, and showed that thickness of dust-free space was about 300 µm for particles of diameter of 0.5 µm when the temperature of the wafer is 30℃ higher than the temperature of air. This result suggested the possibility of controlling particle deposition by thermophoresis, but it did not show how particle deposition flux could be calculated. Turner et al. [1989] performed numerical simulation of particle deposition by considering electrostatic force under the condition of stagnation flow, and pointed out that electrostatic force dominated particle deposition when particle was charged, and that the deposition velocity was reduced to a factor of 1/10-1/100 by eliminating or counterbalancing the electrostatic force. They also proposed that thermophoretic force could be used as counterbalancing force of electrostatic force. In practice, it is hard to eliminate electrostatic force because it is difficult to control or even characterize the particle charge. Donovan et al. [1993] calculated the deposition velocity by adding simply contributions from the five particle transport mechanisms, i.e., sedimentation, diffusion, thermophoresis, electrophoresis and photophoresis, and suggested the decontamination methods by applying controllable thermophoresis, electrophoresis and photophoresis. However, their results and comparison with the experimental data were explained only qualitatively since they simply added the individual contributions.

[†]To whom all correspondences should be addressed.

Experimental investigations on the particle deposition were performed by many investigators in the past. Kuehn [1988] compared the numerical simulation results of air flow field in a cleanroom with the observation of particles transport by injecting small particles into the air stream. From the results, he concluded that the average path of the small particles could be approximated with streamline of air. Therefore, the particle velocity in the convection term of particle mass balance can be substituted with air velocity. Kim and Kim [1991] studied the particle deposition velocity through numerical simulation and experiment considering the thermophoretic and inertia forces on the particles ranging from 0.1 to 30 μm under a stagnant condition. They concluded that the thermophoretic force was dominant when the particle size was below 14 μm, and that inertia force was dominant over 14 μm. Ye et al. [1991] investigated experimentally the thermophoretic effect on the particle deposition from a stagnant flow to the wafer surface, and they suggested that the effective decontamination could be achieved by heating the wafer surface to 10-40℃ over the air temperature for the particle size of below 2 μm. Their results agreed with the results from numerical simulation.

Most of studies dealing with particle deposition have been done on a stagnation flow. In this work, the angle between wafer surface and direction of free-stream flow was introduced as a system parameter, and then numerical simulation was performed on a general flow field. Convection, diffusion, sedimentation, and thermophoresis were included as particle transport mechanisms. It was assumed that the deposition took place on an infinite plane. Similarity transform was applied to the model equations and obtained equations with dimensions reduced by one. Velocity field, temperature profile, and particle concentration profile were obtained by solving numerically momentum balance, energy balance, and particle mass balance. Then particle deposition velocities were examined by varying particle size, temperature difference between wafer surface and air, system pressure, free-stream velocity, and angle between wafer surface and direction of free-stream. From these results, we proposed best strategy to use thermophoretic effect.

MATHEMATICAL FORMULATION

If carrier gas flows to angle of θ with wafer surface as shown in Fig. 1, free-stream velocity is obtained by potential flow theory as follows [Kays and Crawford, 1980].

$$u_\infty = Cx^m \tag{1}$$

where C is a coefficient which makes u_∞ have a velocity unit as m varies, and m is a function of θ giving as follows.

$$m = \frac{\theta/\pi}{1 - \theta/\pi} \tag{2}$$

In this flow field, the boundary-layer momentum equation becomes

$$v\frac{\partial^2 u}{\partial y^2} = u\frac{\partial u}{\partial x} + v\frac{\partial u}{\partial y} + \frac{1}{\rho}\frac{dP}{dx} \tag{3}$$

The pressure gradient term can be expressed in terms of the velocity via the Bernoulli equation as follows.

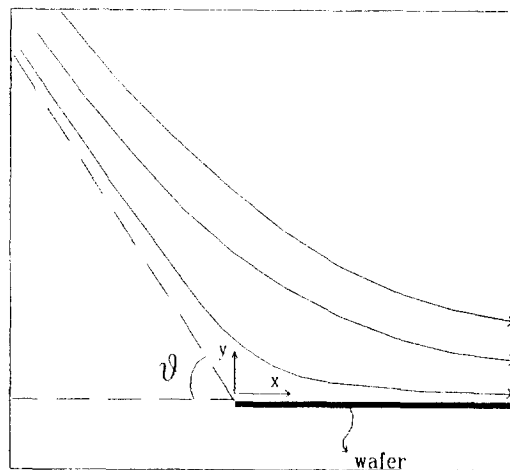$$\frac{dP}{dx} = -\rho Cx^m Cmx^{m-1} = -\frac{\rho u_\infty^2 m}{x} \tag{4}$$

Fig. 1. Schematic diagram of wafer processing system.

Thus

$$v\frac{\partial^2 u}{\partial y^2} = u\frac{\partial u}{\partial x} + v\frac{\partial u}{\partial y} - \frac{u_\infty^2 m}{x} \tag{5}$$

If a variable η is defined for similarity transform as follows,

$$\eta = \frac{y}{\sqrt{vx/u_\infty}} = y\sqrt{\frac{Cx^{m-1}}{v}} \tag{6}$$

then Eq. (5) becomes ordinary differential equation.

$$f''' + \frac{m+1}{2}ff'' + m(1 - f'^2) = 0 \tag{7}$$

where ', ", and '" represent d/dη, $d^2/d\eta^2$, and $d^3/d\eta^3$, respectively, and

$$f'(\eta) = \frac{u}{u_\infty} = \frac{u}{Cx^m} \tag{8}$$

By using continuity equation, we obtain the velocity of y-component.

$$v = -\frac{m+1}{2}(vCx^{m-1})^{1/2}f(\eta) \tag{9}$$

The boundary conditions for momentum equation are as follows.

$$f(0) = 0 \tag{10}$$

$$f'(0) = 0 \tag{11}$$

$$f'(\infty) = 1 \tag{12}$$

If a nondimensional temperature τ is defined as

$$\tau = \frac{T - T_\infty}{T_w - T_\infty} \tag{13}$$

the energy balance equation becomes

$$\alpha\frac{\partial^2 \tau}{\partial y^2} = u\frac{\partial \tau}{\partial x} + v\frac{\partial \tau}{\partial y} \tag{14}$$

The boundary conditions for energy equation are as follows.

$$\tau = 1 \text{ at } y = 0 \tag{15}$$

$$\tau = 0 \text{ at } y \to \infty \tag{16}$$

$$\tau = 0 \text{ at } x = 0 \tag{17}$$

Performing similarity transform for energy equation with η [Eq. (6)] in a similar way to the procedure for momentum equation, the energy equation, Eq. (11), becomes

$$\tau'' + \frac{m+1}{2}\mathrm{Pr}\cdot f\cdot\tau' = 0 \tag{18}$$

Then boundary conditions become

$$\tau(0) = 1 \tag{19}$$

$$\tau(\infty) = 0 \tag{20}$$

If a nondimensional particle concentration φ is defined as

$$\varphi = \frac{c_p}{c_{p,x}} \tag{21}$$

then the particle mass balance equation becomes

$$u\frac{\partial\varphi}{\partial x} + v\frac{\partial\varphi}{\partial y} = D\frac{\partial^2\varphi}{\partial y^2} - \frac{\partial(\varphi V_{th})}{\partial y} - \frac{\partial(\varphi V_{gr})}{\partial y} \tag{22}$$

The gravitational sedimentation velocity V_{gr} is expressed as follows [Reist, 1993].

$$V_{gr} = -\frac{\rho_p d_p^2 g C_c}{18\mu} \tag{23}$$

where d_p is the diameter of particle and C_c is Cunningham's correction factor which is expressed as

$$C_c = 1 + \frac{2.666\times10^3}{Pd_p}[6.32 + 2.01\exp(-8.215\times10^{-4}Pd_p)] \tag{24}$$

where P is absolute pressure in Pa and d_p is the diameter of particle in µm [Reist, 1993]. The gravitational sedimentation velocity decreases with increasing pressure because C_c decreases with increasing pressure. Also C_c decreases with increasing particle size, but gravitational sedimentation velocity increases with increasing particle size because of the d_p^2 term in Eq. (23). Thermophoretic velocity, V_{th} is expressed as follows [Shchukin et al., 1990].

$$V_{th} = -K_T\frac{v}{T}\nabla T \tag{25}$$

where K_T is a thermophoretic coefficient, v is kinematic viscosity, and T is absolute temperature. Therefore, thermophoretic velocity is proportional to temperature gradient and its direction is the direction from high temperature region to low temperature region. Many expressions for thermophoretic coefficient K_T were suggested. In this work, the following expression which is suggested by L. Talbot et al. [1980] is used.

$$K_T = 2.294\frac{(k_a/k_p + 2.2\mathrm{Kn})C_c}{(1 + 3.438\mathrm{Kn})(1 + 2k_a/k_p + 4.4\mathrm{Kn})} \tag{26}$$

where k_a and k_p are thermal conductivities of air and particle, respectively. The ratio of k_a and k_p is negligible because it is very small compared to the other terms. And, Kn is Knudsen number which is defined as $2\lambda/d_p$ where λ is mean free path of air molecule which is expressed as follows [Donovan et al., 1993].

$$\lambda = \frac{\mu}{P}\sqrt{\frac{\mu RT}{2M}} \tag{27}$$

where P is absolute pressure, μ is viscosity of air, and M is average molecular weight of air. From Eq. (26) and Eq. (27), thermo-

phoretic velocity decreases with increasing pressure or particle size because thermophoretic coefficient decreases with increasing pressure or particle size.

The boundary conditions for Eq. (22) are as follows.

$$\varphi = 0 \text{ at } y = 0 \tag{28}$$

$$\varphi = 1 \text{ at } y\to\infty \tag{29}$$

$$\varphi = 1 \text{ at } x = 0 \tag{30}$$

The Eq. (28) is based on the assumption of the instantaneous deposition, i.e., the particles deposit immediately on the wafer surface as soon as they arrive on the surface.

Performing similarity transform with η after neglecting gravitational sedimentation term of Eq. (22), we obtain

$$\frac{1}{Sc}\varphi'' + \left(\frac{K_T\tau'}{\tau+\tau_z} + \frac{m+1}{2}f\right)\varphi' + \frac{K_T}{\tau+\tau_z}\left(\tau'' - \frac{\tau'^2}{\tau+\tau_z}\right)\varphi = 0 \tag{31}$$

where τ_z is a parameter which is related to temperature difference between wafer surface and airflow, and is defined as follows.

$$\tau_z = \frac{T_z}{T_w - T_z} \tag{32}$$

Including gravitational sedimentation term, we obtain the following equation in place of Eq. (31)

$$\frac{1}{Sc}\varphi'' + \left(\frac{K_T\tau'}{\tau+\tau_z} + \frac{m+1}{2}f\right)\varphi' + \frac{K_T}{\tau+\tau_z}\left(\tau'' - \frac{\tau'^2}{\tau+\tau_z}\right)\varphi$$
$$+ \frac{\rho_p d_p^2 g C_c}{18\mu\sqrt{Cv}}\frac{\varphi'}{x^{(m-1)/2}} = 0 \tag{33}$$

Examination of the Eq. (33) reveals that the variable x remains except for the case where m is equal to unity, i.e., stagnation flow. Therefore, ordinary differential equations should be solved at each x positions. Nevertheless, since the ordinary differential equations at each x positions are not dependent on each other, solving Eq. (33) is simpler than to solve the original partial differential equations before performing similarity transform. In a strict sense, the transformation from Eq. (22) to Eq. (33) is simply a transformation from (x, y)-coordinates to (x, η)-coordinates rather than the similarity transform since x is not perfectly eliminated. The boundary conditions for both Eq. (31) and Eq. (33) are as follows.

$$\varphi(0) = 0 \tag{34}$$

$$\varphi(\infty) = 1 \tag{35}$$

It was assumed that temperature of air is 293°K, and diffusivity of particle was calculated by using the following equation [Donovan et al., 1993].

$$D = \frac{kTC_c}{3\pi\mu d_p} \tag{36}$$

Diffusivity of particle decreases with increasing particle size, and decreases with increasing pressure because C_c [Eq. (24)] decreases with increasing pressure. Cunningham's correction factor, thermophoretic coefficient and diffusivity of particle were calculated at 293°K and dependencies of all coefficients on temperature were neglected. Viscosity of air, $1.784\times10^{-4}\mathrm{gcm^{-1}s^{-1}}$, was assumed to be constant at 293°K. Therefore, these physical properties are not dependent on the position, on which the temperature is dependent according to the energy balance equation. And, it was assumed that Prandtl number is equal to unity, particle density
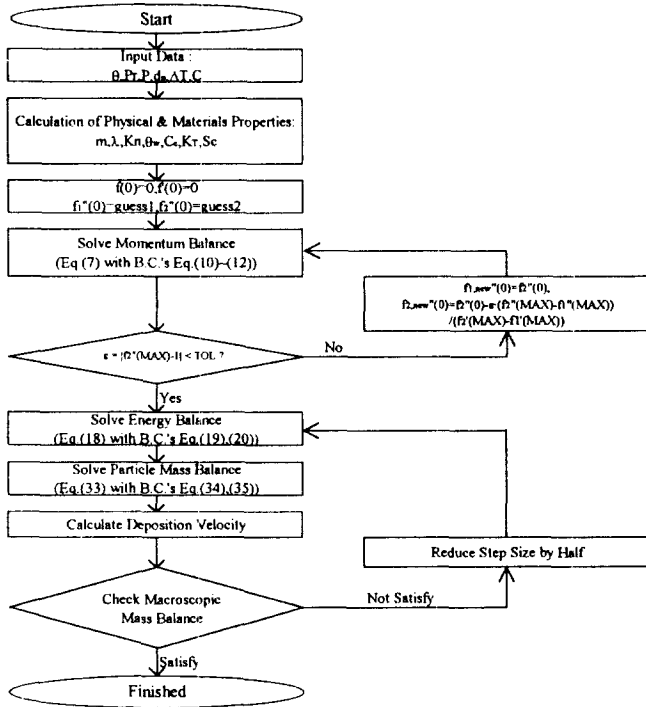
Fig. 2. Flow diagram for numerical calculations.

Fig. 3. Stream lines.
$(\theta = 45°, \ C = 1 \ cm^{2/3}s^{-1})$

Fig. 4. Stream lines.
$(\theta = 90°, \ C = 1 \ cm^{2/3}s^{-1})$

ρ_p is 1 g/cm³, and the length of wafer is 12.5 cm. With these values of physical properties, velocity field was obtained by solving Eq. (7) with boundary conditions Eq. (10)-(12), and then temperature profile was obtained by solving Eq. (18) with boundary conditions Eq. (19) and Eq. (20), and then particle concentration profile was obtained by solving Eq. (33) with boundary conditions Eq. (34) and Eq. (35) (Fig. 2). Discretization of differential equations was done by using finite difference method.

RESULTS AND DISCUSSIONS

The velocity fields around the wafer when the angle of the free-stream to the wafer surface is 45° and 90° were shown in Fig. 3 and 4, respectively. The stream function of the velocity field described by Eq. (7) is given as follows

$$\Psi = \sqrt{vxu_x} \ f(\eta)$$
$$= \sqrt{vCx^{m+1}} \ f(\eta) \qquad (37)$$

In Fig. 3 and Fig. 4, the stream line closest to the wafer surface corresponds to $\Psi = 1$ cm²/s and the stream lines were drawn with an increment of 1 cm²/s. The outer region of the momentum boundary layer was calculated by potential flow theory and the inner region was calculated numerically with Eq. (7). When the free-stream was flowed with an angle of 45° to the wafer surface, the fluid flow in the momentum boundary layer was almost parallel to the wafer surface. However, when it was flowed with an angle of 90°, the velocity component in the y-direction had some value in the momentum boundary layer and consequently the velocity component in the x-direction in the momentum boundary layer was greater than that for the case of 45°. It could be seen from the fact that in Fig. 4, more stream lines were passing through the same cross-sectional area than in Fig. 3.

The temperature profile around the wafer and the concentration profile of the particles were shown in Fig. 5 and 6, respec-
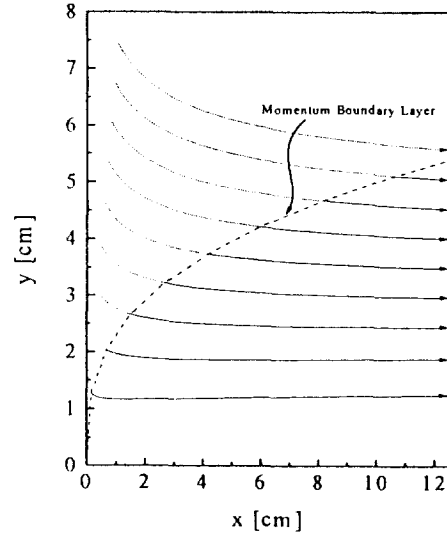
tively. The thermal boundary layer had the same thickness of the momentum boundary layer because the Prandtl number was set to unity. But the concentration boundary layer was much thinner than the momentum boundary layer because the condition of large Schmidt number was considered. In a system where only the diffusion contributes to the particle movement, the thickness ratio of the concentration boundary layer to the momentum boundary layer is proportional to Sc⁻¹/³. When the thermophoresis is significant, it is proportional to Sc⁻¹ [Gokoglu and Rosner, 1985; Gokoglu and Rosner, 1986]. The temperature profile at each position, x, can be transformed completely by similarity transform but the concentration profile cannot be transformed completely. The concentration gradient at x = 1 cm on the wafer surface, at which the concentration boundary layer is thin, is smaller than that at x = 10 cm, at which the concentration boundary layer is thick. It means that the shape of the real concentration boundary layer is different from that used for the numerical calculation, but the
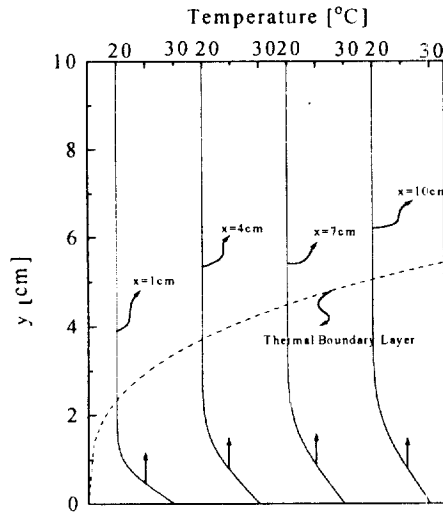
Fig. 5. Temperature profiles.
($\Delta T = 10^\circ C$, $\theta = 45^\circ$, $C = 1$ cm$^{2/3}$s^{-1}, Pr $= 1$)

Fig. 7. Relationship between particle deposition velocity and particle diameter.
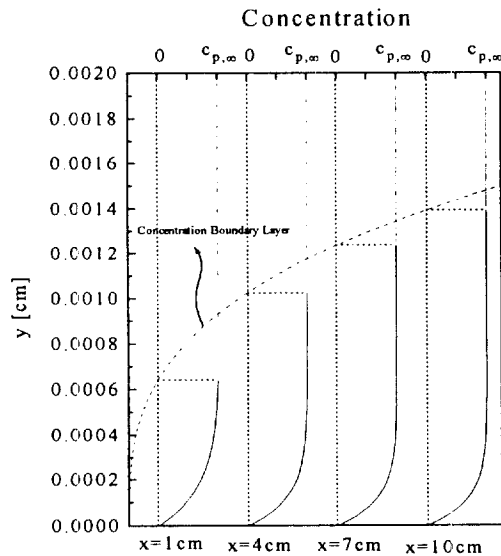($\theta = 90^\circ$, $C = 1$ s^{-1}, $P = 1.013 \times 10^5$ Pa)

Fig. 6. Particle concentration profiles.
($\Delta T = 10^\circ C$, $\theta = 45^\circ$, $C = 1$ cm$^{2/3}$s^{-1}, $d_p = 1$ μm, $P = 1.013 \times 10^5$ Pa)

Fig. 8. Relationship between particle deposition velocity and ΔT.
($\theta = 90^\circ$, $C = 1$ s^{-1}, $P = 1.013 \times 10^5$ Pa)

results of the calculation were not wrong because we chose the thickness of the concentration boundary layer sufficiently thick. This was proved by the smoothness of the concentration profile in the vicinity of the concentration boundary layer.

The deposition velocity of the particles, V_d, which is the main concern of this study, can be written as following equation,

$$V_d = \frac{\text{Total number of moles deposited on the wafer per unit time and unit area}}{\text{particle concentration in the bulk phase}}$$

$$= \frac{\int_0^L N_p(x)dx/L}{c_{b,x}} \tag{38}$$

where N_p and L denote the deposition flux of the particle and length of the wafer, respectively [Bae et al., 1994]. When the
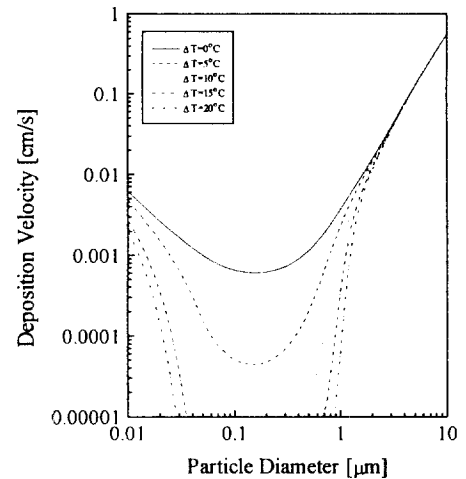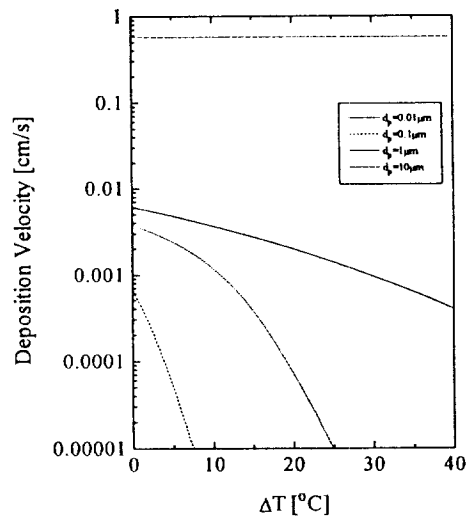
free-stream flows vertically to the wafer, the deposition flux of the particles is independent of x because the concentration profile at each position, x, has a similarity transform and the thickness of the thermal and concentration boundary layers are independent of x. As a consequence, the denominator of Eq. (38) can be simply replaced by N_p. The changes in the deposition velocity of particles were shown from Fig. 7 to 11.

In Fig. 7, the change of deposition velocity with the size of the particles was shown. It can be easily seen that the particles having diameter of 0.1-10 μm are removed efficiently by the thermophoretic effect. Especially, the particles having diameter of around 0.1 μm are removed most efficiently. However, large particles having size of 10 μm are difficult to remove by temperature gradient. This is because, in this regime, deposition by gravity governs the movement of the particles. Likewise, the removal efficiency was lowered for small particles because in this regime diffusion controlled the movement of the particles. The deposition velocities by convective diffusion, thermophoresis and sedimenta-
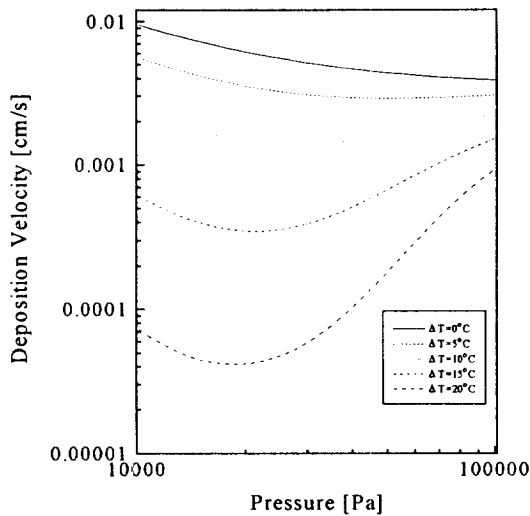
Fig. 9. Relationship between particle deposition velocity and pressure.
$(\theta=60°, C=1 \text{ cm}^{1/2}\text{s}^{-1}, d_p=1 \text{ μm})$

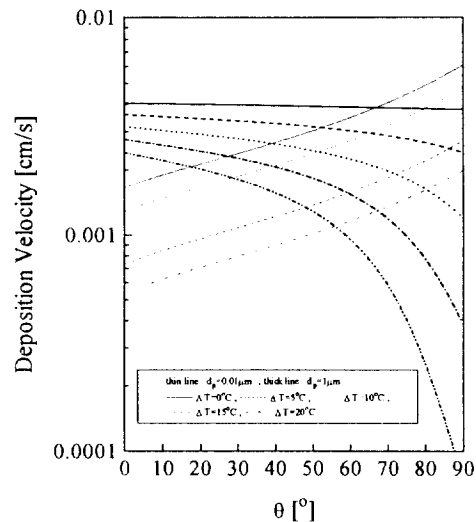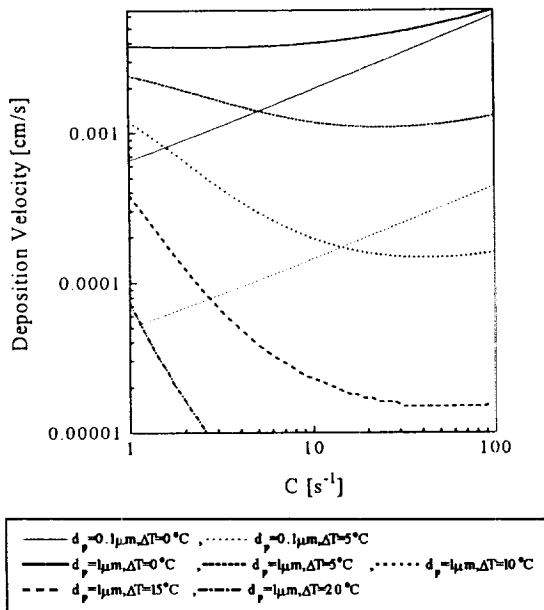Fig. 10. Relationship between particle deposition velocity and C.
$(\theta=90°, P=1.013\times10^5 \text{ Pa})$

tion are expressed as ShD/L ($\simeq Re^{1/2}Sc^{1/3}D/L$), $-K_TvVT/T$ and $\rho_pC_cd_p^2g/18\mu$, respectively [Donovan et al., 1993]. If we calculate the ratio of each contribution when $\theta=90°$, $C=1s^{-1}$, $P=1.013\times10^5$ Pa, and $\Delta T=5°C$, then the relative contribution of convective diffusion, thermophoresis, and sedimentation to the deposition velocity are 1, -2.2×10^{-1}, and 4.1×10^{-2} when the particle diameter is 0.01 μm. As the particle diameter increases to 0.1 μm, 1 μm, and 10 μm, contributions of each mechanisms change to 1: -3.3×10^1: 8.4×10^1, 1: -9.0×10^2: 1.4×10^5, and 1: -2.8×10^3: 2.2×10^8, respectively. These results are consistent with the result that particles smaller than 0.1 μm or larger than 10 μm are difficult to remove by temperature gradient, which is shown in Fig. 7.

In Fig. 8, the change of deposition velocity with the temperature

Fig. 11. Relationship between particle deposition velocity and θ.
$(C=1 \text{ cm}^{1}\text{s}^{-1}, P=1.013\times10^5 \text{ Pa})$

difference between the wafer surface and air flow was shown. The particles having size of 0.1-10 μm are removed well by thermophoresis but the particles which are either very large or very small cannot be easily removed. Especially, the particles of 10 μm are hardly removed by thermophoresis. As referred in the previous parts, the particles which are either very large or very small can be removed by filtration and other techniques. It is very interesting and encouraging that the particles having size of 0.1-1 μm are removed efficiently by thermophoresis because these particles are the contamination source in the industrial semiconductor processing.

In Fig. 9, the change of deposition velocity with pressure was shown. The deposition velocity decreases if there is no temperature difference because both the diffusivity of particle and the sedimentation velocity decrease. But, the range where the deposition velocity increases with increasing pressure exists if temperature difference greater than 5°C are applied to 1 μm sized particles. This range becomes wider as the temperature difference increases. That means, in low pressure processes such as LPCVD, the deposition velocity due to diffusion increases but the effect of thermophoresis can retard the deposition of the particles easily.

In Fig. 10, the change of deposition velocity with the free-stream velocity was shown. Both thermal and concentration boundary layer become thinner if the free-stream velocity increases. As a consequence, diffusion occurs more actively and the deposition velocity of the particles having size of 0.1 μm increase. But, for the 1 μm sized particles on which thermophoresis has greater effect than diffusion, the deposition velocity decreases because the thermophoretic force increases with the free-stream velocity. The deposition velocity increases even for the 1 μm sized particles when the free-stream velocity increases if the condition of no temperature difference is met. The thermophoretic effect is maximized when the free-stream velocity increases if the filter of a cleanroom is carefully designed to remove the particles having size of 0.1 μm. On the contrary, if it removes well the particles having size of 1 μm, the free-stream velocity should be decreased for the thermophoretic effect to be maximized.

In Fig. 11, the deposition velocity of the particles with respect to the angle between the direction of the free-stream and the
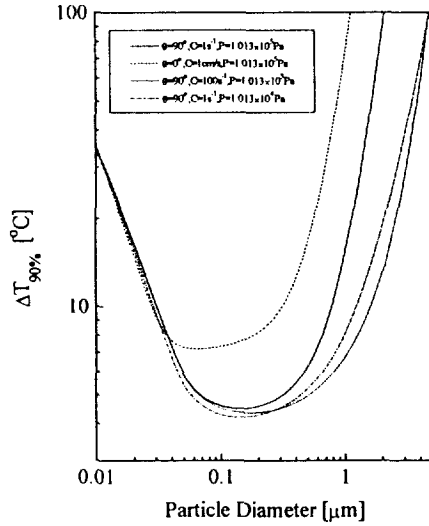
Fig. 12. Relationship between temperature difference for 90% thermophoretic efficiency and particle diameter.

wafer surface was shown. The thicknesses of the thermal and concentration boundary layer become thinner to give the same trend as in Fig. 10 when θ increases just like the case of the free-stream velocity. For the diffusion-controlled 0.01 μm particles, the deposition velocity increases with increasing θ but the 1 μm particles are governed by thermophoresis and the deposition velocity decreases with increasing θ. Consequently, the particle removal efficiency by thermophoresis can be enhanced by adjusting the angle between the free-stream and the wafer surface depending on the characteristics of the filter of the clean room just as the case of the free-stream velocity.

In Fig. 12, the temperature difference between wafer surface and airflow which would give thermophoretic efficiency of 90% depending on the individual size of the particle. The thermophoretic efficiency was defined as follows,

$$(\eta_{Th})_{\Delta T = \Delta T_0} = \left(1 - \frac{V_{d,\Delta T - \Delta T_0}}{V_{d,\Delta T = 0}}\right) \times 100(\%) \qquad (39)$$

When the temperature difference of 40°C is applied, thermophoretic efficiency for particles of diameter ranging from 0.01 to 1.0 μm is higher than or about 90%. However, removing particles, of diameters over 5 μm by thermophoretic effect is practically impossible. From Fig. 12, it can be confirmed that increase of θ or C works favorably for high thermophoretic efficiency, and increase of pressure is against improving thermophoretic efficiency.

CONCLUSIONS

The particle deposition velocities on a wafer were studied under conditions of flows of various angles between wafer surface and the air stream in a cleanroom by numerical simulation. The results suggest that it is plausible to reduce deposition of particles of diameter ranging from 0.1 to 1.0 μm, which are known to be a major problem in micro-electronics industry, by applying a temperature difference of 10-30°C between wafer surface and the air stream.

Particle deposition velocity in LPCVD process is greater than that in APCVD process when the temperature gradient is not

applied. But the efficiency of removing particles by thermophoretic force increases. As the angle between wafer surface and the direction of free-stream, or free-stream velocity increases, thicknesses of both thermal and concentration boundary layer decrease, and then deposition velocity of small particle, which is dominated by diffusional transport, increases, and that of large particle, which is dominated by thermophoretic transport, decreases. Therefore, if the flow angle or free-stream velocity is appropriately controlled according to the design of filter, then the effective removal of particle by thermophoresis can be achieved.

NOMENCLATURE

C : coefficient related to free-stream velocity ($u_\infty = Cx^m$) [m^{1-m} s^{-1}]

C_c : Cunningham's correction factor

c_p : particle concentration inside boundary layer [particles m^{-3}]

$c_{p,\infty}$: particle concentration outside boundary layer [particles m^{-3}]

D : diffusivity of particle in air [$m^2 s^{-1}$]

d_p : diameter of particle [m] ([μm] in Eq. (24))

f′ : dimensionless velocity (f′ = u/u_∞)

g : acceleration of gravity [$m\ s^{-2}$]

Kn : Knudsen number ($2\lambda/d_p$)

K_T : thermophoretic coefficient

k : Boltzman constant [$J\ K^{-1}$]

k_a : thermal conductivity of air [$J\ s^{-1}m^{-1}K^{-1}$]

k_p : thermal conductivity of particle [$J\ s^{-1}m^{-1}K^{-1}$]

L : length of wafer [m]

M : mean molecular weight of air [$kg\ mol^{-1}$]

m : $(\theta/\pi)/(1-\theta/\pi)$

P : absolute pressure [Pa]

Pr : Prandtl number (v/α)

R : gas constant [$J\ mol^{-1}K^{-1}$]

Sc : Schmidt number (v/D)

Sh : Sherwood number

T : temperature inside boundary layer [K]

T_w : temperature at surface of wafer [K]

T_∞ : temperature outside boundary layer [K]

ΔT : temperature difference between wafer and airflow [°]

$\Delta T_{90\%}$: ΔT for 90% removal efficiency [°]

u : velocity of x-direction [$m\ s^{-1}$]

u_∞ : free-stream velocity [$m\ s^{-1}$]

V_d : particle deposition velocity [$m\ s^{-1}$]

V_{gr} : sedimentation velocity by gravitational force [$m\ s^{-1}$]

V_{th} : thermophoretic velocity [$m\ s^{-1}$]

v : velocity of y-direction [$m\ s^{-1}$]

x, y : rectangular coordinates [m]

α : thermal diffusivity of air ($k_a/\rho\hat{C}_P$) [$m^2 s^{-1}$]

η : dimensionless coordinate for similarity transform [$y/(\sqrt{vx/u_\infty})$]

η_{Th} : thermophoretic removal efficiency

θ : angle between wafer surface and free-stream flow [radian]

λ : mean free path of air [m]

μ : viscosity of air [$kg\ m^{-1}s^{-1}$]

v : kinematic viscosity of air [$m^2 s^{-1}$]

ρ : density of air [$kg\ m^{-3}$]

ρ_p : density of particle [$kg\ m^{-3}$]

τ : dimensionless temperature

τ_w : $T_\infty/T_w - T_\infty$

ϕ : dimensionless particle concentration

Ψ : stream function $[m^2 s^{-1}]$

REFERENCES

Bae, G. N., Lee, C. S. and Park, S. O., "Measurement of Particle Deposition Velocity toward a Horizontal Semiconductor Wafer by Using a Wafer Surface Scanner", *Aerosol Sci. & Tech.*, **21**, 72 (1994).

Davis, R. W., Moore, E. F. and Zachariah, M. R., "Numerical Modeling of Particle Dynamics in a Rotating Disk Chemical Vapor Deposition Reactor", *J. Crystal Growth*, **132**, 513 (1993).

Donovan, R. P., Yamamoto, T., Periasamy, R. and Clayton, A. C., "Mechanisms of Particle Transport in Process Equipment", *J. Electrochem. Soc.*, **140**(10), 2917 (1993).

Gokoglu, S. A. and Rosner, D. E., "Thermophoretically Augmented Mass Transfer Rates to Solid Walls across Laminar Boundary Layers", *AIAA J.*, **24**(1), 172 (1985).

Gokoglu, S. A. and Rosner, D. E., "Prediction and Rational Correlation of Thermophoretically Reduced Particle Mass Transfer to Hot Surfaces Across Laminar or Turbulent Forced-convection Gas Boundary Layers", *Chem. Eng. Commun.*, **44**, 107 (1986).

Harrigan, J. and Stoller, M., "Automated Wafer Inspection in the Manufacturing Line", *Solid State Tech.*, **Oct.**, 69 (1991).

Kays, W. M. and Crawford, M. E., "Convective Heat and Mass Transfer", McGraw-Hill, New York (1980).

Kim, Y. J. and Kim, S. S., "Particle Size Effects on the Particle Deposition from Non-isothermal Stagnation Point Flows", *J. Aerosol Sci.*, **22**(2), 201 (1991).

Kuehn, T. H., "Predicting Air Flow Patterns and Particle Contamination", *J. Aerosol Sci.*, **19**(7), 1405 (1988).

Reist, P. C., "Aerosol Science and Technology", McGraw-Hill, New York (1993).

Shchukin, E. R., Shulimanova, Z. L., Zagaynov, V. A. and Kabanov, A. N., "Deposition of Aerosol Particles in Plane-parallel Channels at Different Wall Temperatures", *J. Aerosol Sci.*, **21**(2), 189 (1990).

Stratmann, F., Friedlander, S., Fissan, H. and Papperger, A., "Suppression of Particle Deposition to Surfaces by the Thermophoretic Force", *J. Aerosol Sci.*, **18**(6), 651 (1987).

Talbot, L., Cheng, R. K., Schefer, R. W. and Willis, D. R., "Thermophoresis of Particles in a Heated Boundary Layer", *J. Fluid Mech.*, **101**(4), 737 (1980).

Turner, J. R., Liguras, D. K. and Fissan, H. J., "Clean Room Applications of Particle Deposition from Stagnation Flow: Electrostatic Effects", *J. Aerosol Sci.*, **20**(4), 403 (1989).

Ye, Y., Pui, D. Y. H., Liu, B. Y. H., Opiolka, S., Blumhorst, S. and Fissan, H., "Thermophoretic Effect of Particle Deposition on a Free Standing Semiconductor Wafer in a Clean Room", *J. Aerosol Sci.*, **22**(1), 63 (1991).